

Blind Shear-Wave Velocity Comparison of ReMi and MASW Results with Boreholes to 200 m in Santa Clara Valley: Implications for Earthquake Ground-Motion Assessment

by W. J. Stephenson, J. N. Louie, S. Pullammanappallil, R. A. Williams, and J. K. Odum

Abstract Multichannel analysis of surface waves (MASW) and refraction microtremor (ReMi) are two of the most recently developed surface acquisition techniques for determining shallow shear-wave velocity. We conducted a blind comparison of MASW and ReMi results with four boreholes logged to at least 260 m for shear velocity in Santa Clara Valley, California, to determine how closely these surface methods match the downhole measurements. Average shear-wave velocity estimates to depths of 30, 50, and 100 m demonstrate that the surface methods as implemented in this study can generally match borehole results to within 15% to these depths. At two of the boreholes, the average to 100 m depth was within 3%. Spectral amplifications predicted from the respective borehole velocity profiles similarly compare to within 15% or better from 1 to 10 Hz with both the MASW and ReMi surface-method velocity profiles. Overall, neither surface method was consistently better at matching the borehole velocity profiles or amplifications. Our results suggest MASW and ReMi surface acquisition methods can both be appropriate choices for estimating shear-wave velocity and can be complementary to each other in urban settings for hazards assessment.

Introduction

Shallow shear-wave velocity (V_s) has long been recognized as a key factor in variable ground-motion amplification and site response in sedimentary basins (Borcherdt, 1970). It is an important parameter in building codes (NEHRP, 1997), and the earthquake engineering community widely uses V_s in design applications (Kramer, 1996). Hazards-mapping methodology is advancing to more accurately incorporate local V_s information into the hazards calculation, in particular, in urbanized areas (Cramer, 2003; Cramer *et al.*, 2004). This trend is expected to accelerate with future expansion of these efforts (Applegate, 2004). Incorporation of scenario earthquakes into future hazard characterization will also depend on reliable V_s determinations in the upper several hundred meters. As such, the need to rapidly and inexpensively determine shallow V_s over large urban sedimentary basins will become critical to accurately represent site response in future urban hazard maps. In general, borehole logging is considered the standard for obtaining V_s data, but drilling and logging to the depths generally required for earthquake ground-motion investigations is very expensive, and it is becoming increasingly problematic in heavily urbanized settings. This, in part, has led to the development of numerous surface acquisition techniques to obtain shallow V_s . The spatial autocorrelation (SPAC) and frequency-wave

number (FK) methods, which rely on surface acquisition and analysis of microtremors, were some of the earliest developed to derive V_s (an overview of these methods is given by Okada, 2003). These methods have been useful in resolving V_s in the upper several kilometers (Okada, 2003). Conventional active-source seismic reflection/refraction has also been used extensively for shallow V_s characterization to 50 m (Williams *et al.*, 2003). More recently, the spectral analysis of surface waves (SASW) method has been widely used for shallow V_s characterization (Stokoe and Nazarian, 1985; Brown *et al.*, 2002). Each of these methods has been successful to varying degrees in replicating results obtained by borehole measurements.

Multichannel analysis of surface waves (MASW) (Park *et al.*, 1999), and refraction microtremor (ReMi) (Louie, 2001), are two of the techniques that have been developed most recently for determining shallow V_s . Both have similar data acquisition requirements by primarily using traditional seismic reflection/refraction equipment. Both MASW and ReMi acquisition utilize a linear array of vertically oriented sensors, which makes them ideally suited for investigators already equipped to do near-surface engineering reflection/refraction seismology. Depth of investigation for both is primarily a function of array length and resonant sensor fre-

quency, although in the case of MASW source energy is also a key factor. The resonant sensor frequency and the signal source primarily govern bandwidth. MASW and ReMi differ fundamentally in their recorded source signal type. MASW is an active-source technique requiring an impulsive signal, such as from a sledgehammer or weight drop, or swept vibratory signal, such as vibroseis, to generate surface waves. V_s structure is typically derived from the fundamental mode Rayleigh wave field generated by the source. ReMi, conversely, is a passive technique, recording ambient noise or microtremors ubiquitous in the urban environment. V_s is derived by identifying the fundamental mode Rayleigh wave field within the microtremors.

Four boreholes drilled to depths between 260 and 413 m within the Evergreen and Cupertino basins in the Santa Clara Valley, California, were logged for S -wave velocity using a P - S suspension technique (Wentworth *et al.*, 2003; Fig. 1). The four logs generally show V_s ranging between 200 m/sec and 1300 m/sec, typical for the upper few hundred meters in young sedimentary basins. The GUAD well is unique among these four because it bottomed in hard rock and, unfortunately, the upper 50 m were not logged because of well casing (C. Wentworth, personal comm., 2003). The rapid variability in V_s with depth at each of the respective boreholes is believed to be geologically meaningful and not suspension log measurement noise (C. Wentworth, personal comm., 2004). Numerous previous studies have compared surface acquisition methods with borehole V_s logs (Boore and Brown, 1998; Liu *et al.*, 2000; Brown *et al.*, 2002; Williams *et al.*, 2003). This study compares V_s depth models derived from MASW and ReMi techniques at these four logged boreholes to evaluate their depth of investigation and robustness in an urban environment. Differences in V_s are then investigated by comparing predicted ground amplification for these methods at each borehole.

Data Analysis

A principal reason for this investigation is to determine whether the noninvasive MASW and ReMi surface seismic methods can reasonably estimate the shear-wave velocity structure in the upper few hundred meters at a site and, therefore, can be used with some confidence in estimating site-amplification effects for earthquake hazards. Thus, we simulate a real-world scenario, where MASW or ReMi are used to acquire V_s data without prior knowledge of borehole velocities. To this end, we interpret all data “blind” such that the interpretations presented here were finalized prior to the first inspection of the borehole logs. Acquisition parameters were selected to maximize the potential depth of investigation at the expense of detailed structure in the upper 5–10 m. ReMi data were analyzed independently by three of the authors and interpreted by forward modeling (J. N. L. and S. P.) and by an inversion technique (W. J. S.).

The ReMi data were acquired at each of the four sites with 4.5-Hz vertical geophones and 5-m receiver spacing.

Lower natural-frequency sensors would potentially be better but were unavailable. Array length depended on the available geographic space at each site, but ranged from 200 to 295 m. Data consisted of 10–20 ambient noise records of 30 sec length transformed to the slowness–frequency (p - f) domain (McMechan and Yedlin, 1981) and stacked prior to dispersion analysis, as described by Louie (2001). All acquired ReMi records were used in the p - f analysis unless amplitudes within a given record were clipped. A typical noise record and p - f domain image of ReMi data is displayed in Figure 2. The greatest difficulty in analyzing these data is in picking the frequency–slowness points representing the dispersion curve. Because the ReMi method relies on a linear receiver array, there is no obvious way to distinguish noise arrival azimuth. Therefore apparent phase velocities picked on spectral peaks in the p - f domain image may be artificially high. In general, Louie (2001) recommends picking two extremal dispersion curves (one at low-phase velocity along the threshold where the spectra departs from incoherent noise and one along the spectral peaks, as shown in Fig. 2b) and at a third “best guess” dispersion curve along or near the top of the steep spectral gradient between the extremals.

MASW data were acquired with the identical receiver array as the ReMi data. Published studies using MASW tend to be for detailed shallow 2D V_s profiles (Park *et al.*, 1999, Miller *et al.*, 2000), for which it is well suited. The goal here is to seek greater depth and not be greatly concerned with mapping spatial variability. We used a 250-kg accelerated weight drop to generate surface waves. The MASW records selected for analysis in this study were from off-end source locations. If coherent surface waves were present in a given raw-field record, that record was utilized in the p - f analysis. Whereas ReMi data required no preprocessing before transformation into the p - f domain, MASW data first required field stacking as well as a geometric gain correction and often benefited from trace muting of all wave phases extraneous to the surface waves. A typical X-T domain MASW field record is shown after gain correction in Figure 3a. It primarily contains fundamental and higher-mode surface waves along with coherent urban noise. The p - f domain analysis technique for MASW data was almost identical with that of ReMi, with the primary difference being where the dispersion curve was picked on the p - f spectral image, as shown in Figure 3b. Because the source of the surface-wave energy is known, the fundamental-mode amplitude peak is assumed to be the correct dispersion-curve location. The higher-mode surface wave is very distinct in the p - f domain at this site. Although higher modes were not analyzed in this study, exploiting them might prove valuable in future studies.

The weight drop source generated higher-frequency surface-wave energy, as indicated by the strong coherent amplitude ridge above 12 Hz, than was generally observed in the microtremor data (Fig. 2b). Conversely, the weight drop often lacked low-frequency signal below 4 Hz, which generally limited the maximum depth of investigation of the

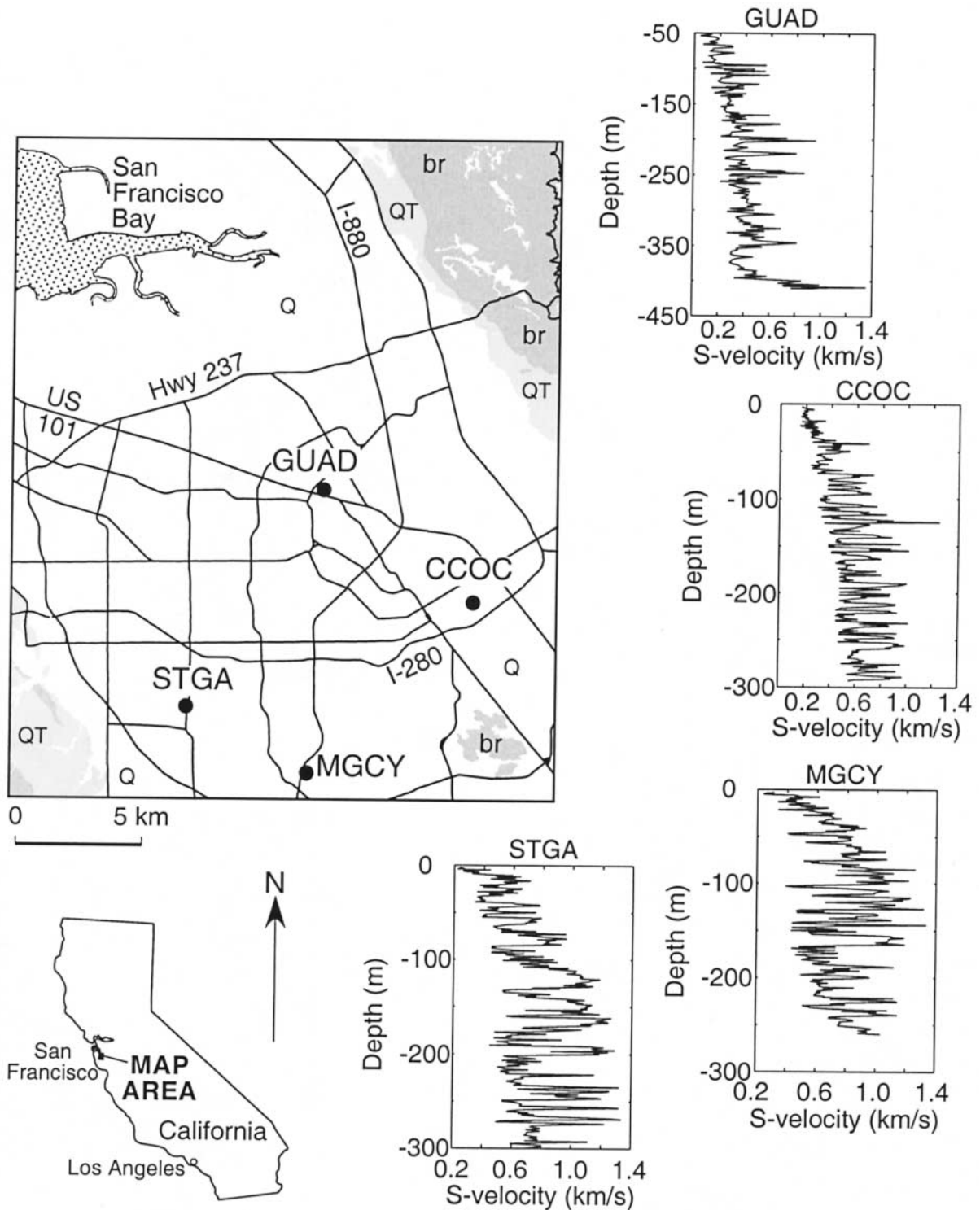


Figure 1. Well locations investigated in the Santa Clara Valley, south of San Francisco Bay, California. Simplified geologic units are labeled as follows: br, bedrock (undifferentiated); QT, undifferentiated Quaternary/Tertiary deposits; Q, Holocene/Pleistocene deposits. S-wave velocity suspension logs for boreholes CCOC, GUAD, MGCY, and STGA are shown at the right. Map modified from C. Wentworth (personal comm., 2003).

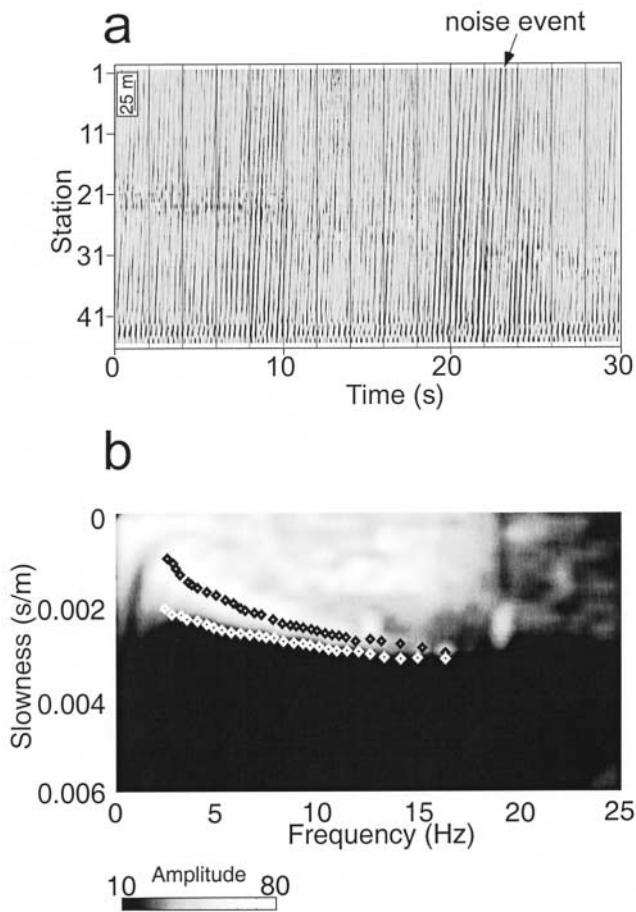


Figure 2. (a) A typical noise record acquired by the ReMi technique in Santa Clara Valley. In general, 10–20 records, each 30 sec long, were acquired at each site. (b) A p-f image of ReMi data acquired at MGCY with two extremal dispersion curves picked (black and white diamonds).

MASW method as it was implemented in this study. A different source, such as a controlled-vibration device or larger accelerated mass, might potentially produce a lower-spectral content and therefore increase the depth of investigation.

Inverse Modeling of ReMi and MASW Data

We used the iterative least-squares 1D inverse routine of Herrmann and Ammon (2002) for modeling velocity profiles using the dispersion curves interpreted from both the ReMi and MASW data. This software was chosen because of its free availability and its general use within the seismological community (Malagnini *et al.*, 1995). The data were inverted “blind,” before the borehole data were viewed, to avoid any modeling bias. The inversion code required an initial model of layers, layer thicknesses, V_s , V_p/V_s ratio (or V_p), and density. Synthetic testing showed that a reasonable initial model was important to the final inverted result. In general, our initial ReMi models were set to be a uniform

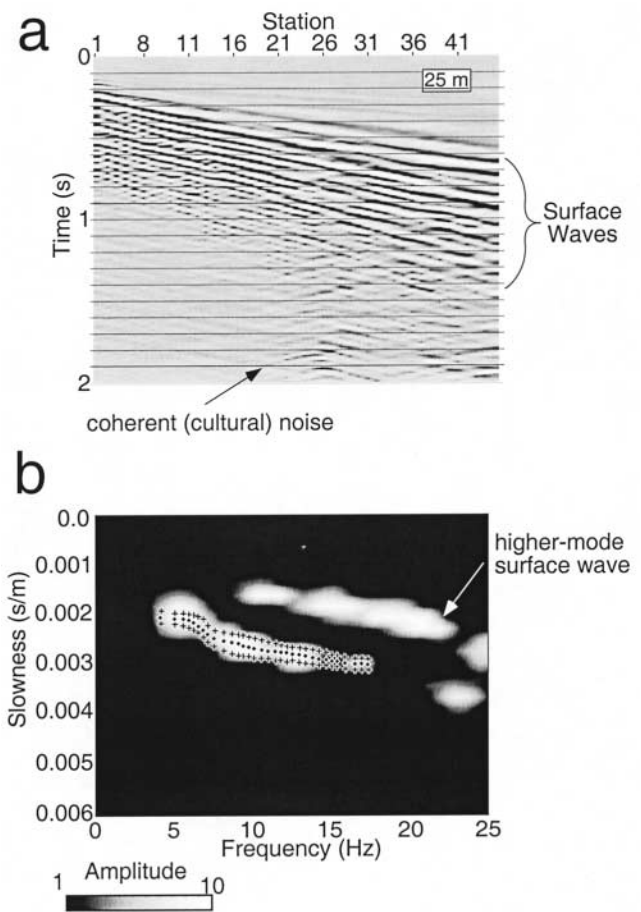


Figure 3. (a) A typical weight drop record acquired by the MASW technique in Santa Clara Valley. Cultural noise is seen contaminating this record, particularly between 1 and 2 sec, between stations 22 and 30. (b) A p-f image of MASW data acquired at MGCY with upper- and lower-bound dispersion curves shown as black crosses; the peak dispersion curve is shown with black diamonds.

half-space, including 20 layers at the top, each of 10-m thickness. Initial MASW models were set up identically except that layer thicknesses were 5 m to reflect the generally higher-frequency dispersion picks in these data. All initial shear velocities were set to a visually inspected average of the picked phase velocities. More sophisticated layering in the initial models might have improved the final solutions, but building in *a priori* assumptions would have departed from the “blind” hypothesis. The number of dispersion data points ranged between 30 and 50, depending on the data set. Maximum modeling depths were estimated using suggested guidelines discussed by Park *et al.* (1999) and approximated by the equation

$$z_{\max} = \frac{C_1}{2 * f_1}$$

where Z_{\max} is the maximum depth, f_1 is the lowest analyzed frequency, and C_1 is the phase velocity at that frequency.

Previous studies have suggested that Rayleigh dispersion curves are much more sensitive to S -wave than to P -wave shallow velocity structure (Xia *et al.*, 1999; Liu *et al.*, 2000; Louie, 2001). Because the code of Herrmann and Ammon (2002) requires either setting V_p or V_p/V_s for each inverted layer, V_p/V_s ratios were set to a constant of 2. Although this is probably not an accurate value for shallow deposits at the four sites, the S -wave velocity inversion results were relatively insensitive to this parameter, as the previous studies have described.

We picked two extremal dispersion curves on the ReMi p-f images for each site (e.g., MGCY is shown in Fig. 2b). The high-velocity extremal picks are on the apex of the slowest coherent ridge and the low picks are near the base of this ridge on the low-velocity (high slowness) side. Qualitatively, the low extremal approximates the phase velocities of microtremors from the ends of the array, whereas the high extremal estimates phase velocities arriving at high angles of incidence relative to the array orientation. Each dispersion curve was inverted separately, and the geometric mean of the resulting velocity models was calculated for the final solution. The geometric mean was used because it is less affected than other mean estimates by large variations in the extremal solutions. Ultimately, incorporating extremal dispersion bounds into the modeling is designed to account for the azimuthal uncertainty of the microtremor arrivals.

Three MASW dispersion curves were picked and inverted for each dataset. The preferred solution was inverted from dispersion picks along the slowest high-amplitude ridge in each p-f image (e.g., for MGCY in Fig. 3b). Upper- and lower-bound dispersion curves were also picked and inverted to help estimate variability. Standard deviation of the solution was derived from the three inverted solutions, departing on average by 6% (MGCY), 10% (GUAD), 12% (STGA), and 30% (CCOC) from preferred. Some deviations reached as high as 55% at depths greater than 50 m (CCOC).

Forward Modeling, ReMi Data

In addition to the inversion of the ReMi data described previously, two of the authors (J. N. L. and S. P.) forward-modeled these data for an independent and blind comparison with both the borehole and the inversion results. Louie (2001) describes the analysis (identical through the p-f domain transformation to the inverse solutions of W. J. S.) and modeling methodology in detail. Forward modeling was performed with the proprietary software package SeisOpt[®] ReMi[™] (Optim Software, Inc.; with modeling based on Saito, 1979 and 1988).

For this component of the blind comparison, both data analysis and modeling were undertaken independently by authors J. N. L. and S. P. in the absence of any knowledge of the location or description of the four sites. Author

W. J. S. provided J. N. L. and S. P. with raw microtremor data files and array-spacing parameters, with the sites identified only by the letters A–D. Author J. N. L. combined the two blind forward analyses for each borehole into a single preferred solution and transmitted them, along with models representing estimated variance, to W. J. S. who prepared the comparative text and figures presented here.

The independent forward modeling followed the methods of Louie (2001) as well as those outlined previously by picking high- and low-velocity extremal dispersion curves for each site. A “best-guess” or preferred curve was also picked. For each site the preferred curve first was forward-modeled by hand in the manner described by Louie (2001); the velocity is set for the surface layer by modeling the shortest-period phase-velocity picks, and the modeling proceeds downward. The number and depths of interfaces are modeled to match the occurrence of phase-velocity gradients in the dispersion curve. Velocity inversions are not inserted unless demanded by a reversal or a high gradient in the dispersion curve. With the number of interfaces and their depths modeled from the preferred dispersion curve, incremental adjustments are usually sufficient to model the extremal dispersion curves, providing estimates of model variance. This modeling procedure requires less than 1 hr per site with the SeisOpt[®] ReMi[™] package.

Borehole-Surface Methods Velocity Comparison

Resulting V_s curves at each study site are compared against the respective borehole log in Figure 4. Maximum depths of investigation varied from site to site and only the portion of each borehole log above that respective maximum depth is displayed for clarity. By inspection, each of the surface-method solutions is a reasonable first-order match with the borehole velocity profile. Except that the inverse-modeled results tend to be smoother than the forward-modeled results, no clear systematic method bias can be discerned in these comparisons. Yet, as pointed out by Boore and Brown (1998), comparison by visual inspection is an unsatisfactory approach because it is both subjective and qualitative. To obtain a more quantitative comparison, and following NEHRP guidelines, we use the formula

$$V_{S_z} = \frac{\sum_{i=1}^n d_i}{\sum_{i=1}^n (d_i/V_{S_i})}$$

to calculate statistical measures of V_s as a function of depth. In this formula, V_{S_z} is the average shear-wave velocity to a depth of Z meters, d_i is the thickness of the i th individual layer, and v_i is the interval velocity of that layer (NEHRP, 1997). We calculate the borehole averages using the unfiltered velocity logs, although using an effective media approximation, such as Backus averaging (Backus, 1962),

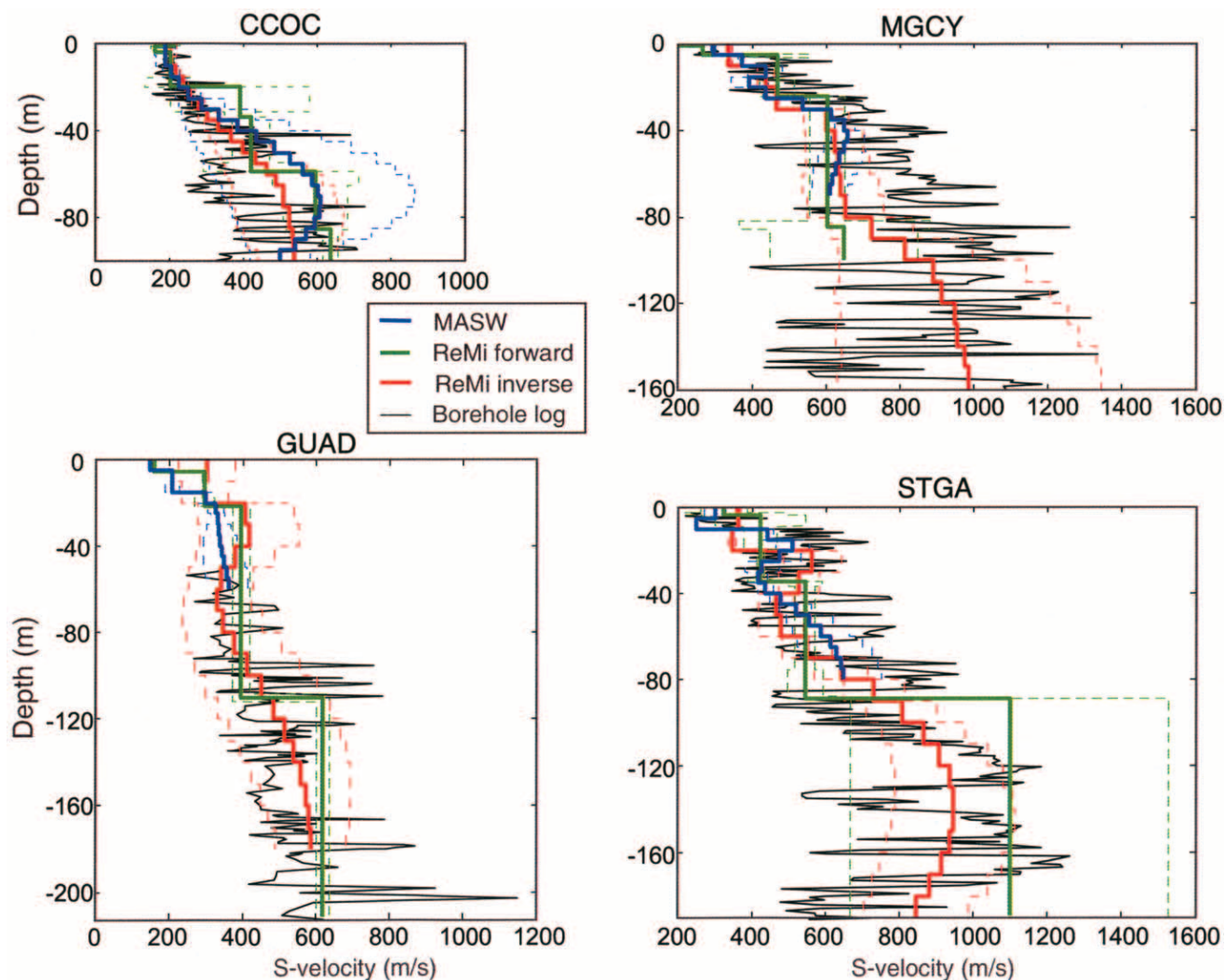


Figure 4. Suspension borehole shear-wave velocity logs (thin black lines) compared with surface methods. MASW inverse results are heavy blue lines, ReMi forward results are heavy green lines, and ReMi inverse results are heavy red lines. Blue and red dashed lines are the estimated standard deviation for MASW and ReMi inverse models, respectively, based on extremal modeling results. Green dashed lines are the estimated standard deviation for ReMi forward model results, as calculated by author W. J. S. from the suite of models submitted by authors J. N. L. and S. P.

Table 1
CCOC Velocity Estimators
(Percent Difference from Borehole in Parentheses)

Velocity Estimator	Borehole	ReMi Forward (J.N.L.)	MASW	ReMi Inverted (W.J.S.)
V_s 30	206	238 (15)	220 (7)	230 (12)
V_s 50	248	287 (16)	268 (8)	266 (7)
V_s 100	301	381 (27)	365 (21)	348 (16)

Table 2
MGCY Velocity Estimators
(Percent Difference from Borehole in Parentheses)

Velocity Estimator	Borehole	ReMi Forward (J.N.L.)	MASW	ReMi Inverted (W.J.S.)
V_s 30	444	412 (-7)	398 (-10)	406 (-9)
V_s 50	515	473 (-8)	469 (-9)	469 (-9)
V_s 100	638	530 (-17)	—	560 (-12)

Table 3
STGA Velocity Estimators
(Percent Difference from Borehole in Parentheses)

Velocity Estimator	Borehole	ReMi Forward (J.N.L.)	MASW	ReMi Inverted (W.J.S.)
V_s 30	409	408 (-1)	376 (-8)	404 (-2)
V_s 50	430	444 (3)	405 (-6)	436 (1)
V_s 100	505	515 (2)	496 (-2)	511 (1)

Table 4
GUAD Velocity Estimators
(Percent Difference from Borehole in Parentheses)

Velocity Estimator	Borehole	ReMi Forward (J.N.L.)	MASW	ReMi Inverted (W.J.S.)
V_s 30	—	273	245	328
V_s 50	—	312	300	353
V_s 100*	346	349 (1)	—	356 (3)

*Calculated only over interval 50–100 m.

would also give an appropriate comparative average. Tables 1 to 4 list the respective average of the methods at each borehole. The GUAD borehole does not have a 30- or 50-m average because the suspension log is absent to 50 m (because of well casing). V_s 30 was chosen for comparison because it is traditionally the guideline value imposed in the building codes. V_s 50 was selected because this depth was consistently reached in all surface-method interpretations at the boreholes. V_s 100 was reached in a majority of interpretations and is included as a deeper end-member estimate for these data.

All surface-method interpretations at borehole CCOC overestimate the three V_s averages relative to the borehole, ranging from 7 to 15% for V_s 30, from 7 to 16% for V_s 50, and from 16 to 27% for V_s 100. There is a velocity inversion at CCOC between 52 and 75 m depth that none of the surface-method interpretations resolve, and this is expressed as a particularly poor fit in the V_s 100 estimate (Table 1). The dispersion data did not require a velocity inversion for a reasonable fit by ReMi forward modeling. Of the three surface-method solutions, the inverted ReMi result compared most closely overall, although MASW fared best with the V_s 30 estimate.

At borehole MGCY, all methods underestimate V_s relative to the borehole velocities, between 7 and 10% for V_s 30, between 8 and 9% for V_s 50, and between 12 and 17% for V_s 100 (Table 2). MASW results at MGCY can only be interpreted to about 65 m depth and are not included in this V_s 100 error range. The ReMi forward and inverse solutions were slightly better in the V_s 30 and V_s 50 estimates than was MASW. MGCY showed the strongest overall velocity gradient with depth, as well as the largest variations; for example, with velocity increasing by a factor of 3 from 140 to 145 m depth. With both surface acquisition methods mea-

suring surface-wave propagation in low-velocity channels, little energy within the measured frequency band samples the highest velocities.

The best statistical fit in this study occurred at borehole STGA, where all methods underestimate V_s 30 by 1 to 8%, misestimate V_s 50 by 1 to 6%, and misestimate V_s 100 by 1 to 2%. Again, ReMi tended to be slightly better by this comparison than MASW. This is partially because the MASW data were severely degraded at this site by automobile traffic that overwhelmed much of the active-source signal.

The only usable estimate for the GUAD borehole is V_s 100, and this is estimated only over the interval 50–100 m. ReMi interpretations match very well from 50 to 100 m depth, overestimating by 1 to 2%. As at MGCY, MASW data did not sample to sufficiently low frequency to obtain V_s 100 at GUAD. For the shallower velocities, the values from forward ReMi are between the MASW and inverted ReMi values.

Predicted Ground-Motion Amplification

Ground amplification predicted for a V_s velocity structure is ultimately what is important in assessing the viability of a surface acquisition technique for ground-motion assessment. Using the relative site-amplification analysis method of Boore and Brown (1998), we compare predicted differences in amplification using the V_s profiles of the boreholes and our surface methods. This method is partially based on the quarter wavelength approximation of Joyner *et al.* (1981) that forms amplification ratios of different velocity models. It does not account for resonance from high seismic impedance boundaries. Rather, it gives an amplification curve that is essentially a smoothed version of the exact theoretical amplification (Boore and Brown, 1998). The program RATTLE (C. S. Mueller, U.S. Geological Survey, written comm., 1997) has also been suggested as an alternative for this amplification modeling. Boore and Brown (1998) give a comparison of these two modeling approaches. All amplification curves in Figure 5a are relative to a theoretical rock site of 2 km/sec shear velocity and 2600 kg/m³ density. Each amplification curve is calculated from 1 to 20 Hz, every 0.5 Hz. Because GUAD was not logged from 0 to 50 m, we calculate amplification both at 50 m depth (dashed lines, Fig. 5a) and at the surface, assuming a constant velocity from 0 to 50 m depth.

The amplification curves are normalized to the respective borehole result in Figure 5b. In general, curves match best between 2 and 8 Hz at sites CCOC, MGCY, and STGA, at which frequencies surface waves are sampling deeper. This effect is possibly a function of the acquisition parameters that emphasized depth over shallow resolution. The GUAD site appears limited to 4 Hz and less at the surface level because of the absence of the 50-m log interval and to 8 Hz at the 50-m depth level. No amplification at 50 m depth was calculated for MASW data. All surface-method solutions underpredict relative to the CCOC borehole, which is consistent with the overestimation of V_s noted previously.

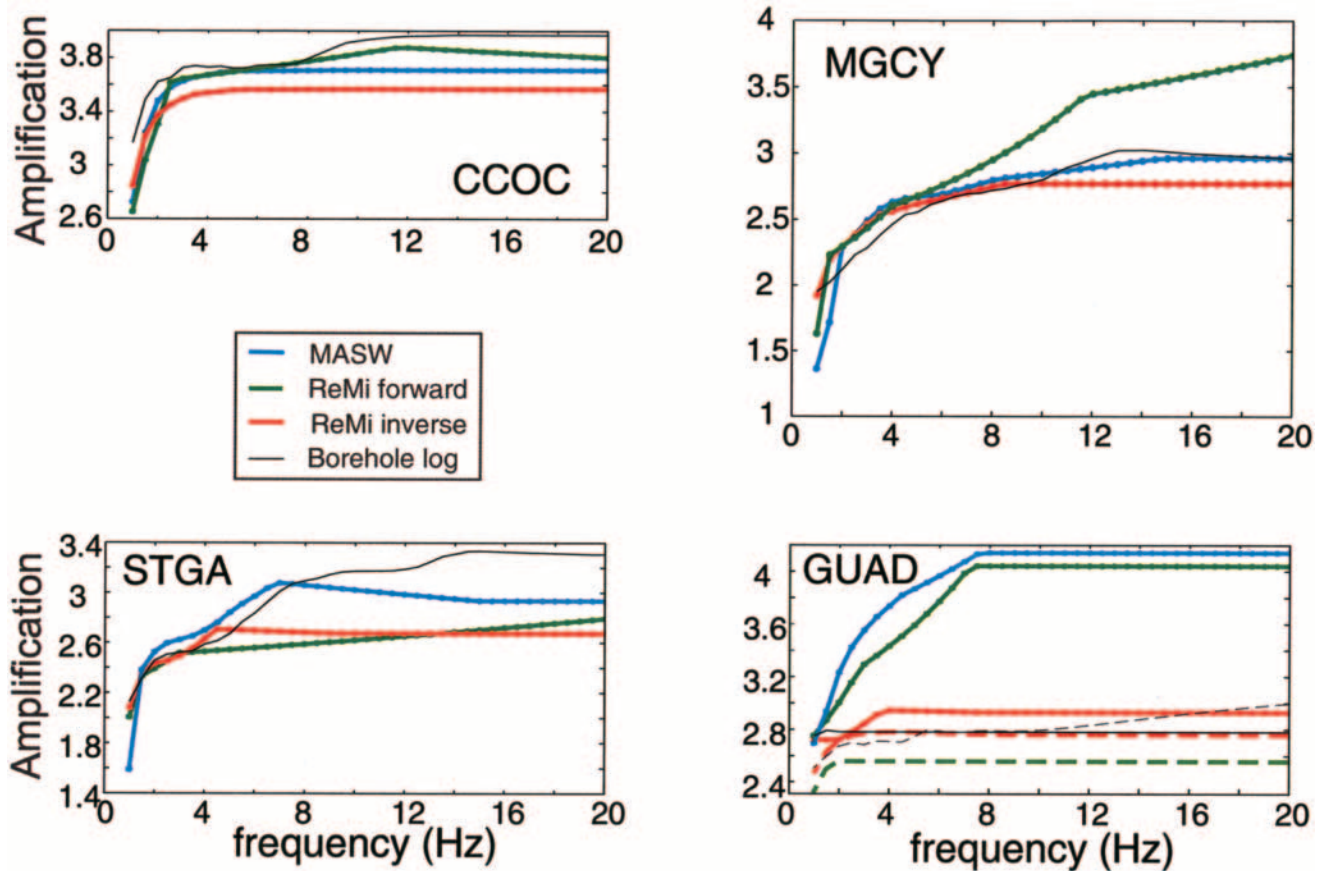


Figure 5. (a) Comparison of spectral amplification from borehole V_s with ReMi and MASW methods. Amplification is predicted relative to a common theoretical rock site. Amplification at GUAD shown at ground surface (solid lines) and at 50 m depth (dashed lines). (b) Ratio of surface method spectral amplifications to borehole spectral amplification. Amplification at GUAD shown at ground surface (solid lines) and at 50 m depth (dashed lines). All vertical axes are displayed at the same scale. (continued)

The inversion results, by the nature of the least-squares inversion algorithm, tend to be smoothed representations of velocity, whereas the forward-modeled results tend to have fewer layers and higher impedance contrasts across boundaries (Fig. 4). The relative shapes of the amplification curves are not dramatically different at any of the sites (Fig. 5b), so the modeling methodology as implemented in this study does not seem to cause dramatic differences to the predicted spectral shapes (this would probably not be the case using a program such as RATTLE). Differences in predicted amplification of the surface methods at sites CCOC, MGCY, and STGA are all within 10% of the respective boreholes between 2 and 8 Hz. Predicted amplifications are within 5% for ReMi curves between 1.5 and 5 Hz at STGA. A similar predicted-amplification percentage was obtained for the MASW and ReMi inverse curves from 5.5 to 11.5 Hz at MGCY.

Discussion and Conclusions

The MASW and ReMi results compared favorably to the boreholes using the three statistical velocity estimators, but

there are plausible factors that could introduce systematic error in this comparison. For example, additional detailed acquisition focusing on the upper 10 m might allow better constraint on both the forward and inverse models at depth. Some of the modeling procedures utilized in this blind comparison can also introduce error. A more sophisticated initial inverse model with variable layer thickness might have led to a more accurate modeling solution, as might more accurate *a priori* V_p/V_s information. Although dispersion is most sensitive to changes in V_s as previously discussed, Brown (1998) documented that differences in V_s of 20% are possible if V_p/V_s is grossly misestimated. Louie (2001) suggests no higher than 10% differences in V_s are possible even with a “huge” variation in Poisson ratio. Other modeling factors such as the assumption of 1D layering can also introduce error.

It is possible that a significant distance between the borehole and surface acquisition locations contributed to differences in the V_s estimations because of variations in subsurface lithology. Surface-method acquisition at sites CCOC and MGCY was hundreds of meters from the boreholes

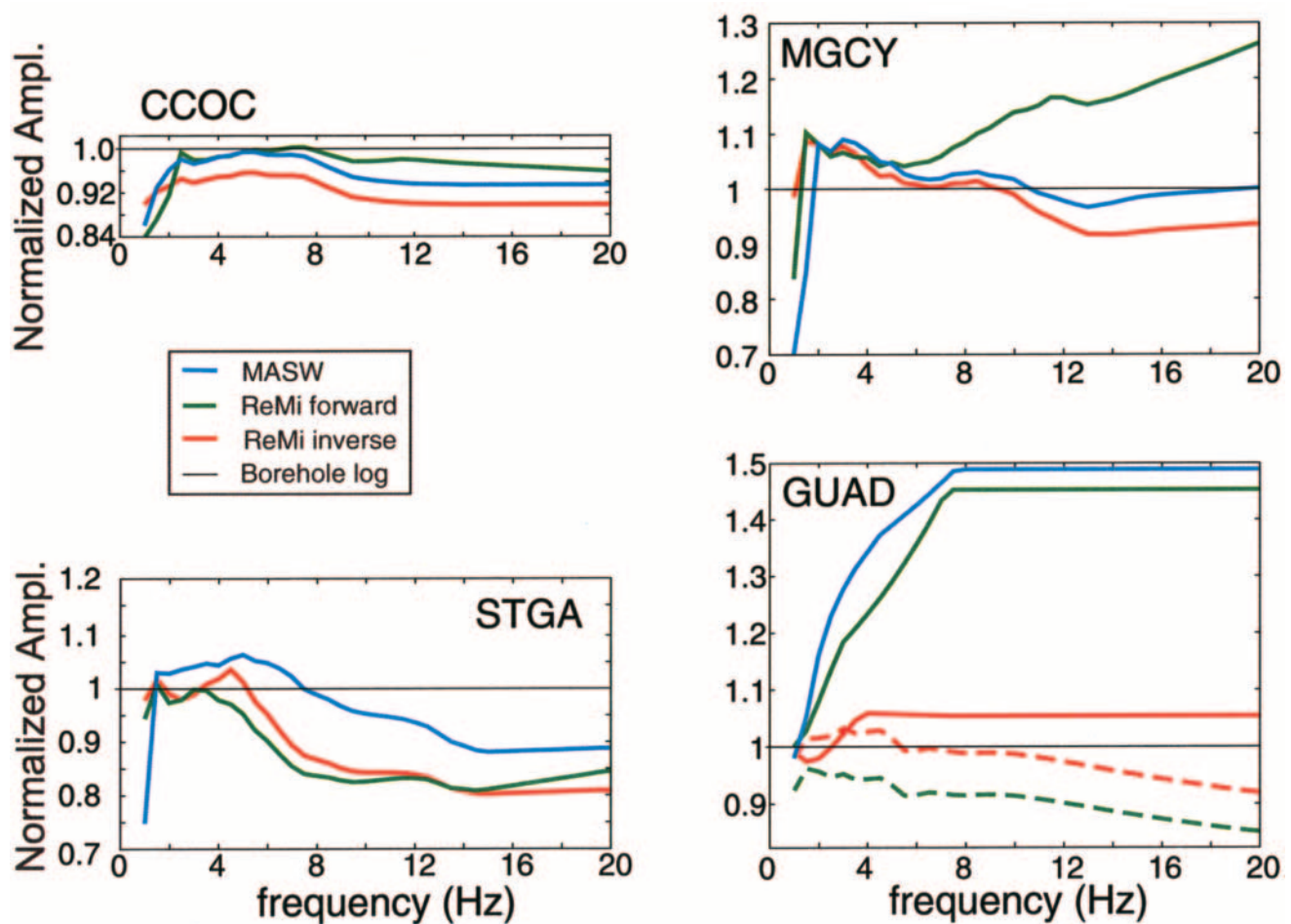


Figure 5. Continued.

(greater than an array length), whereas acquisition at STGA and GUAD took place with at least one array sensor within 20 m of the respective borehole. If lithologic variability plays a role, then one might expect more error introduced at CCOC and MGCY. Tables 1 to 4 suggest STGA and GUAD are statistically closer to their respective borehole velocity profiles than CCOC or MGCY, although there is only minor correlative improvement at STGA in predicted amplification (Fig. 5b). More difference (error) is probably due to the nature of the acquisition methods, with boreholes sampling a very detailed but localized area and surface methods being affected by a larger bulk sample of material.

Yet another source of error could be shear-wave anisotropy, which alone can lead to 10–15% velocity differences between vertically and horizontally propagating waves in the same media (Sheriff, 1984). Borehole measurements are conducted vertically using body waves, whereas the surface methods relied on surface waves traveling horizontally, presumably with elliptical particle motion. Although the relationship between body-wave and surface-wave anisotropy in shallow sedimentary basins is most likely complex, there has been work suggesting these phenomena are related at deep crustal/upper mantle depths (Montagner and Griot-

Pommer, 2000). It is conceivable that a notable percentage of difference (although probably not 15%) may be due simply to travel path differences for the analyzed seismic wavefield.

As part of the overall modeling process, picking dispersion curves for ReMi data is perhaps less intuitive than for MASW data. Because the arrival azimuth of the velocity energy is not known in the ReMi method, Louie (2001) states “picking is done along a lowest-velocity envelope bounding the energy.” At a given frequency, this velocity envelope is defined between the low-phase velocity, where the p-f domain spectral ratio just begins to depart from incoherent noise, and the high-phase velocity along the spectral-ratio peak (Fig. 2). This envelope dispersion-picking procedure is generally followed for both the forward and inverse modeling in this article. Through modeling these extremal dispersion curves, Louie (2001) noted “this procedure will produce extremal velocity profiles at the limits of the velocity range allowed by the dispersion data,” with 95–99% of the velocity energy of interest in the p-f domain usually falling between the picked velocity extremes.

Standard deviations of the interpreted models in Figure 4, in general, suggest that model resolution decreases with

depth, as might be expected for surface-wave dispersion techniques, which are inherently nonunique. Resolution particularly degrades with depth at MGCY and STGA. Each of the four boreholes was at a site with a thick unconsolidated to semiconsolidated stratigraphic section that had no dramatic impedance contrasts (e.g., shallow bedrock) logged above 400 m. As such, these sites may be conducive to generally favorable results with surface-wave dispersion techniques. A similar type of investigation in an area of more complicated media (e.g., higher shallow velocity contrasts and more extreme velocity gradients) may not be as well suited for similar results.

Given the 250-kg weight drop source, the MASW method did not generally image as deep as ReMi at the four investigated sites. This might be primarily because of the source and acquisition parameters used at the four sites. Because MASW has the flexibility to use sources of differing bandwidth, field procedures could potentially be tailored to image the upper 30 m in more detail. In a heavily trafficked urban area, tailoring the field procedures of the ReMi technique could also result in recovery of additional shallow detail, because urban microtremors can also have a broad spectrum. ReMi data acquisition is easier and more time efficient, requiring less equipment than MASW; however, adding MASW source points to a ReMi array did not increase acquisition time dramatically. Both methods would have benefited from lower natural-frequency sensors for deeper imaging.

Numerous surface methods have been developed and utilized to obtain V_s in the upper several hundred meters. Results of this blind comparison study in Santa Clara Valley, California, support the use of ReMi and MASW in urban areas as viable techniques for obtaining V_s to as deep as 100 m, a depth important for earthquake hazards assessment. At three of the sites, ReMi data could be interpreted to at least 160 m. Overall, neither acquisition method investigated here was consistently better at matching the borehole velocity profiles or predicted amplifications, but results obtained from both are complementary and make a good “cross-check” of the solutions.

Acknowledgments

We are greatly indebted to David Worley for his assistance during data acquisition. Special thanks to Randy Hanson and Carl Wentworth for supplying the S -velocity logs used in this investigation. Funding was provided by the National Earthquake Hazards Reduction Program (NEHRP), with partial support from external contract no. 03HQGR006D (to J.N.L.). This manuscript was greatly improved by reviews from Leo Brown, Art Frankel, Steve Hartzell, and an anonymous reviewer.

Use of trade names is for descriptive purposes only and does not represent a product endorsement by the U.S. Geological Survey.

References

- Applegate, D. (2004). Opinion: stepping up to the plate, *Seism. Res. Lett.* **75**, 335–337.
- Backus, G. E. (1962). Long-wave elastic anisotropy produced by horizontal layering, *J. Geophys. Res.* **67**, 4427–4440.
- Boore, D. M., and L. T. Brown (1998). Comparing shear-wave velocity profiles from inversion of surface-wave phase velocities with downhole measurement: systematic differences between the CXW method and downhole measurement at six USC strong motion sites, *Seism. Res. Lett.* **69**, 222–229.
- Borcherdt, R. D. (1970). Effects of local geology on ground motion near San Francisco Bay, *Bull. Seism. Soc. Am.* **60**, 29–61.
- Brown, L. T. (1998). Comparison of V_s profiles from SASW and borehole measurements at strong motion sites in southern California, *Master's Thesis*, University of Texas at Austin, 349 pp.
- Brown, L. T., D. M. Boore, and K. H. Stokoe, II (2002). Comparison of shear-wave slowness profiles at 10 strong-motion sites from non-invasive SASW measurements and measurements made in boreholes, *Bull. Seism. Soc. Am.* **92**, 3116–3133.
- Cramer, C. H. (2003). Site-specific seismic hazard analysis that is completely probabilistic, *Bull. Seism. Soc. Am.* **93**, 1841–1846.
- Cramer, C. H., J. S. Gomberg, E. S. Schweig, B. A. Waldron, and K. Tucker (2004). The Memphis, Shelby County, Tennessee, Seismic Hazard Maps, U.S. Geol. Surv. 2004-1294.
- Herrmann, R. B., and C. J. Ammon (2002). Computer Programs in Seismology, version 3.20: Surface Waves, Receiver Functions, and Crustal Structure, St. Louis University, Missouri.
- Joyner, W. B., R. E. Warrick, and T. E. Fumal (1981). The effect of Quaternary alluvium on strong ground motion in the Coyote Lake, California, earthquake of 1979, *Bull. Seism. Soc. Am.* **71**, 1333–1349.
- Kramer, S. L. (1996). *Geotechnical Earthquake Engineering*, Prentice-Hall, Upper Saddle River, New Jersey.
- Liu, H. P., D. M. Boore, W. B. Joyner, D. H. Oppenheimer, R. E. Warrick, W. Zhang, J. C. Hamilton, and L. T. Brown (2000). Comparison of phase velocities from array measurements of Rayleigh waves associated with microtremors and results calculated from borehole shear-wave velocity profiles, *Bull. Seism. Soc. Am.* **90**, 666–678.
- Louie, J. N. (2001). Faster, better: shear-wave velocity to 100 meters depth from refraction microtremor arrays, *Bull. Seism. Soc. Am.* **91**, 347–364.
- Malagnini, L., R. B. Herrmann, G. Biella, and R. de Franco (1995). Rayleigh waves in Quaternary alluvium from explosive sources: determination of shear-wave velocity and Q structure, *Bull. Seism. Soc. Am.* **85**, 900–922.
- McMechan, G. A., and M. J. Yedlin (1981). Analysis of dispersive waves by wave field transformation, *Geophysics* **46**, 869–874.
- Miller, R. D., C. B. Park, J. Ivanov, J. Xia, D. R. Lafien, and C. Gratton (2000). MASW to investigate anomalous near-surface materials at the Indian Refinery in Lawrenceville, Illinois, Kansas Geological Survey Open-File Rept. 2000-4.
- Montagner, J. P., and D. A. Griot-Pommera (2000). How to relate body wave and surface wave anisotropy, *J. Geophys. Res.* **105**, 19,015–19,027.
- National Earthquake Hazards Reduction Program (NEHRP) (1997). *NEHRP Recommended Provisions for Seismic Regulations for New Buildings and Other Structures, Part 1: Provisions*, Building Seismic Safety Council, Washington, D.C.
- Okada, H. (2003). *The Microtremor Survey Method*, Geophysical Monograph Series, no. 12, Society of Exploration Geophysicists, Tulsa, Oklahoma, 135 p.
- Park, C. B., R. D. Miller, and J. Xia (1999). Multichannel analysis of surface waves, *Geophysics* **64**, 800–808.
- Saito, M. (1979). Computations of reflectivity and surface wave dispersion curves for layered media; I, Sound wave and SH wave, *Butsuri-Tanku* **32**, no. 5, 15–26.
- Saito, M. (1988). Compound matrix method for the calculation of spheroidal oscillation of the Earth, *Seism. Res. Lett.* **59**, 29.
- Sheriff, R. E. (1984). *Encyclopedic Dictionary of Exploration Geophysics*, Society of Exploration Geophysicists, Tulsa, Oklahoma.

- Stokoe, K. H., II, and S. Nazarian (1985). Use of Rayleigh waves in liquefaction studies, in *Proc. Conf. On Measurement and Use of Shear Wave Velocity for Evaluating Dynamic Soil Properties*, Denver, Colorado, 1 May 1985, R. D. Woods (Editor), American Society of Civil Engineers, New York.
- Wentworth, C. M., R. T. Hanson, M. Newhouse, R. C. Jachens, E. A. Mankinen, G. Phelps, J. C. Tinsley, C. F. Williams, R. A. Williams, D. W. Andersen, and E. P. Metzger (2003). Stratigraphy and hydrogeology of the Santa Clara Valley, San Francisco Bay region, California: a progress report, in *American Association of Petroleum Geologists, Pacific Section, Conference Program and Abstracts*, May 19–24, Long Beach, California, p. 94.
- Williams, R. A., W. J. Stephenson, and J. K. Odum (2003). Comparison of P- and S- wave velocity profiles obtained from surface seismic refraction/reflection and downhole data, *Tectonophysics* **368**, 71–88.
- Xia, J. R., R. D. Miller, and C. B. Park (1999). Estimation of near-surface shear-wave velocity by inversion of Rayleigh waves, *Geophysics* **64**, 691–700.
- U.S. Geological Survey
Box 25046, MS 966
Denver, Colorado 80225
wstephens@usgs.gov
(W.J.S., R.A.W., J.K.O.)
- Nevada Seismological Laboratory
Mackay School of Earth Science and Engineering
University of Nevada
Reno, Nevada 89557
louie@seismo.unr.edu
(J.N.L.)
- Optim LLC
Reno, Nevada 89557
satish@optimsoftware.com
(S.P.)

Manuscript received 15 December 2004.